AD

TECHNICAL REPORT ARCCB-TR-92046

NONDESTRUCTIVE EVALUATION OF ELECTRODEPOSITED CHROMIUM

MARK E. TODARO

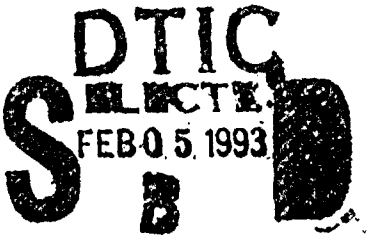

NOVEMBER 1992

US ARMY ARMAMENT RESEARCH,
DEVELOPMENT AND ENGINEERING CENTER
CLOSE COMBAT ARMAMENTS CENTER
BENÉT LABORATORIES
WATERVLIET, N.Y. 12189-4050

DISCLAIMER

The findings in this report are not to be construed as an official Department of the Army position unless so designated by other authorized documents.

The use of trade name(s) and/or manufacturer(s) does not constitute an official indorsement or approval.

DESTRUCTION NOTICE

For classified documents, follow the procedures in DoD 5200.22-M, Industrial Security Manual, Section II-19 or DoD 5200.1-R, Information Security Program Regulation, Chapter IX.

For unclassified, limited documents, destroy by any method that will prevent disclosure of contents or reconstruction of the document.

For unclassified, unlimited documents, destroy when the report is no longer needed. Do not return it to the originator.

REPORT DOCUMENTATION PAGE

Form Approved
OMB No. 0704-0188

1. AGENCY USE ONLY (Leave blank)	2. REPORT DATE	3. REPORT TYPE AND DATES COVERED
	November 1992	Final

4. TITLE AND SUBTITLE
NONDESTRUCTIVE EVALUATION OF ELECTRODEPOSITED CHROMIUM

5. FUNDING NUMBERS
AMCMS: 611102H61001
PRON: 1A03ZOCANMSC

6. AUTHOR(S)
Mark E. Todaro

7. PERFORMING ORGANIZATION NAME(S) AND ADDRESS(ES)
U.S. Army ARDEC
Benet Laboratories, SMCAR-CCB-TL
Watervliet, NY 12189-4050

8. PERFORMING ORGANIZATION REPORT NUMBER
ARCCB-TR-92046

9. SPONSORING / MONITORING AGENCY NAME(S) AND ADDRESS(ES)
U.S. Army ARDEC
Close Combat Armaments Center
Picatinny Arsenal, NJ 07806-5000

10. SPONSORING / MONITORING AGENCY REPORT NUMBER

11. SUPPLEMENTARY NOTES
Presented at the 39th Defense Conference on Nondestructive Testing, Modesto, CA, 5-9 November 1990. Published in the Proceedings of the Conference.

12a. DISTRIBUTION / AVAILABILITY STATEMENT
Approved for public release; distribution unlimited

12b. DISTRIBUTION CODE

13. ABSTRACT *(Maximum 200 words)*

Benet Laboratories is pursuing methods for nondestructively evaluating the quality and adhesion of electrodeposited chromium coatings on the bore of large caliber gun tubes. The Army currently has no suitable means for testing such coatings nondestructively. A poor quality or poorly adherent coating shows up only when several test rounds are fired through the tube, removing portions of the coating and exposing the steel underneath. Recent in-house work has investigated both photothermal and ultrasonic methods. The photothermal method involves briefly heating the surface of the chromium with a laser pulse. After the initial heating, the surface temperature decreases as heat diffuses into the coating and substrate. The characteristics of the coating, interface, and substrate affect the surface temperature profile in distinct ways. The temperature of the surface can be measured by observing the emitted infrared radiation with a focused detector or an infrared scanner. Although no experimental data using the photothermal technique has been obtained yet, a one-dimensional finite difference algorithm was used to model temperature changes on the surface of a chromium coating on steel due to an incident energy pulse. The model verifies that with a suitable choice of laser pulse width, one could measure the thermal characteristics of the coating and detect the presence of a thermal discontinuity at the interface. In the ultrasonic approach, we are attempting to detect and measure interference between ultrasonic stress waves reflected from a chromium-substrate interface and from a chromium-air interface. For a normal, well-bonded coating on steel, little or no reflection would be expected from the chromium-steel interface due to the similarity in characteristic impedances; however, a poor bond or a low density coating could result in enough of an impedance discontinuity to allow significant reflection. Thus far, no interference effects have been observed for chromium on steel, on highly oxidized steel, or on copper.

14. SUBJECT TERMS	15. NUMBER OF PAGES
Chromium, Nondestructive Evaluation, Coatings, Photothermal, Ultrasound, Ultrasonic	10
	16. PRICE CODE

17. SECURITY CLASSIFICATION OF REPORT	18. SECURITY CLASSIFICATION OF THIS PAGE	19. SECURITY CLASSIFICATION OF ABSTRACT	20. LIMITATION OF ABSTRACT
UNCLASSIFIED	UNCLASSIFIED	UNCLASSIFIED	UL

TABLE OF CONTENTS

List of Illustrations

INTRODUCTION

Electrodeposited chromium is currently the material of choice for protecting the bores of large caliber guns from erosion and corrosion. Two basic types of coatings are popular: high contraction (HC) and low contraction (LC). HC chromium has been used successfully for many years despite its high density of microcracks. LC chromium, slightly more ductile and deposited without cracks, has become more popular in recent years. This study is concerned principally with LC chromium.

In the past, variations in the electrodeposition process led to adhesion problems that appeared during test firing. During the firing of test rounds, many tubes experienced the loss of significant amounts of chromium. exposing portions of the underlying steel. Statistical quality control techniques have been successfully applied to the electrodeposition process, leading to improved performance. Under some circumstances, however, a technique for nondestructive evaluation of the coating is still desirable. The Army currently lacks any such nondestructive evaluation techniques for hard, protective coatings in general. Ultimately, this work could lead to the development of techniques applicable to chromium and many other similar coatings.

The work described herein involves both photothermal and ultrasonic techniques.

PHOTOTHERMAL TECHNIQUE

This study investigated the effect of rapidly and briefly heating the surface of a chromium coating using a pulsed heat source such as a laser. Similar results for thermally sprayed coatings have been reported by P. Cielo (ref 1). The subsequent cooling of the surface depends on the coating, substrate, and interface properties. Although no actual measurements were taken, we developed a computer program to model such transient surface temperature profiles due to an energy pulse incident on the surface of a layered material. The program uses a simple one-dimensional finite difference algorithm to model the diffusion of heat into the coating and substrate, neglecting heat loss at the surface. It has been used to predict temperature versus time profiles for a number of different situations involving a chromium coating on steel. The model is used for guiding, analyzing, and interpreting experimental work with the pulsed photothermal technique.

Analytical Solution For a Semi-Infinite Solid

First, we consider a case in which the diffusion equation can be solved analytically: a semi-infinite solid. Suppose an instantaneous pulse of heat is absorbed at the surface of a semi-infinite solid and that the solid loses no heat at the surface. In other words, to a first approximation, we shall neglect cooling of the surface by radiation, air convection, or conduction and consider only diffusion into the material. Since the material is semi-infinite, the diffusion is then one-dimensional. The change in surface temperature T due to the heat pulse as a function of time t after the pulse is (ref 2)

$$T(t) = \frac{Q}{\sqrt{\pi \rho c k t}} \qquad (1)$$

where Q is the energy absorbed per unit area, ρ is the density, c is the specific heat, and k is the thermal conductivity. As a result, ln(T) plotted versus ln(t) will yield a straight line of slope -1/2.

If the heat pulse is continuous rather than instantaneous, then the surface temperature T as a function of time t from the beginning of the pulse is given by

$$T(t) = \frac{1}{\sqrt{\pi \rho c k}} \int_0^t \frac{q(t')dt'}{\sqrt{t-t'}} \qquad (2)$$

where q(t) is the energy absorbed per unit area per unit time. For the simple case of a rectangular pulse given by

$$\begin{aligned} q(t) &= S \qquad 0<t<t_{off} \\ &= 0 \qquad t>t_{off} \end{aligned} \qquad (3)$$

the result simplifies to

$$T(t) = \frac{2S}{\sqrt{\pi \rho c k}} \sqrt{t} \qquad 0<t<t_{off} \qquad (4a)$$

$$T(t) = \frac{2S}{\sqrt{\pi \rho c k}} \left(\sqrt{t} - \sqrt{t - t_{off}}\right) \qquad t>t_{off} \qquad (4b)$$

Finite Difference Solution for Layered Material

In general, if the material is layered with varying thermal properties as a function of depth, an analytical solution is no longer possible. In this case, a one-dimensional finite difference algorithm can be used to find approximate values for the temperature change at the surface or at various depths. Following Dusinberre's treatment (ref 3), we can subdivide the system into regions as shown schematically in Figure 1.

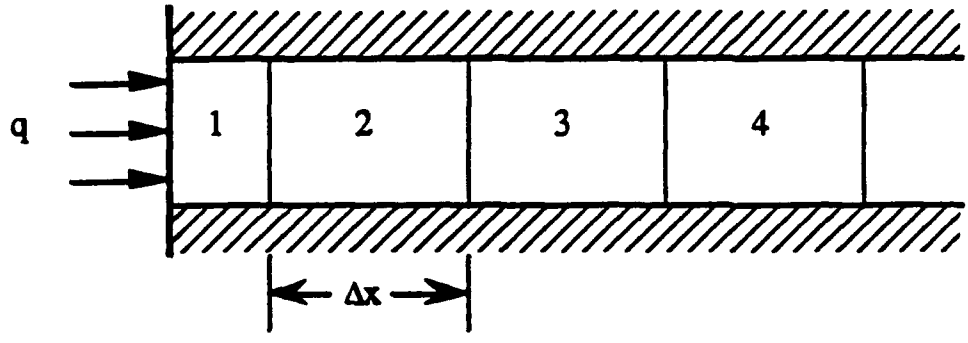

Figure 1. One-dimensional system for finite difference calculations.

The first region has a thickness $\Delta x/2$; all other regions have a thickness Δx. The temperature T_i' for the i^{th} region after each time interval Δt is calculated from the temperatures of the adjacent regions before the time interval using

$$T_1' = \frac{4k_2}{k_1 + k_2}\frac{1}{M_1}T_2 + \left(1 - \frac{4k_2}{k_1 + k_2}\frac{1}{M_1}\right)T_1 + \frac{2\Delta t}{\rho_1 c_1 \Delta x}q \qquad \textbf{(5a)}$$

and for i > 1,

$$T_i' = \frac{2k_{i-1}}{k_{i-1}+k_i}\frac{1}{M_i}T_{i-1} + \frac{2k_{i+1}}{k_i+k_{i+1}}\frac{1}{M_i}T_{i+1} + \left[1 - \left(\frac{2k_{i-1}}{k_{i-1}+k_i} + \frac{2k_{i+1}}{k_i+k_{i+1}}\right)\frac{1}{M_i}\right]T_i \qquad \textbf{(5b)}$$

where

$$M_i = \frac{\rho_i c_i (\Delta x)^2}{k_i \Delta t} \qquad \textbf{(6)}$$

where q is the energy absorbed per unit area per unit time. An arbitrary time-varying energy input can be approximated by using different values of q for each time interval. Typically, q is set to finite values for a "pulse on" period, then to zero for the rest of the calculation. The best results are obtained when each M is greater than or equal to 2.

Computational Results

For a rectangular energy input pulse incident on a semi-infinite homogeneous solid, the finite difference calculations agreed quite well with the analytical solution given by Eq. (4).

The finite difference program was used to model temperature profiles for a variety of different energy pulses and coating systems. Figure 2 shows the results for 50, 200, and 900 μs rectangular pulses incident on three different coating systems: 137.5 μm chromium on steel, 135.7 μm "low density" chromium on steel, and 112.5 μm chromium on a 25 μm "thermal barrier" on steel. The normal properties of chromium used were thermal conductivity of 0.94 W/(cm C), specific heat of 0.448 J/(g C), and density of 7 g/cm^3. The low density chromium was assumed to have a density of 5.1 g/cm^3. The thermal barrier had the same specific heat and density as chromium, but had one-tenth the thermal conductivity. The properties of steel used were thermal conductivity of 0.7 W/(cm C), specific heat of 0.5 J/(g C), and density of 7.8 g/cm^3. In all cases, the total energy density of the pulse was assumed to be 1 J/cm^2. The time step Δt was 5 μs, and the element thickness Δx was 25 μm.

As seen in Figure 2, the shortest energy pulse is best for distinguishing the three coating systems. The 200 μs pulse is just as good as the 50 μs pulse for distinguishing the thermal barrier system from the other two, but not as good for distinguishing the low density coating from the normal density one. In general, the shorter the energy pulse, the better the ability to resolve variations of properties with depth. However, for a given total energy density, the shorter pulses will compress this energy into a shorter time interval, resulting in higher intensities and higher surface temperatures. At the higher energies and shorter times available with many of today's pulsed lasers, surface melting could easily result.

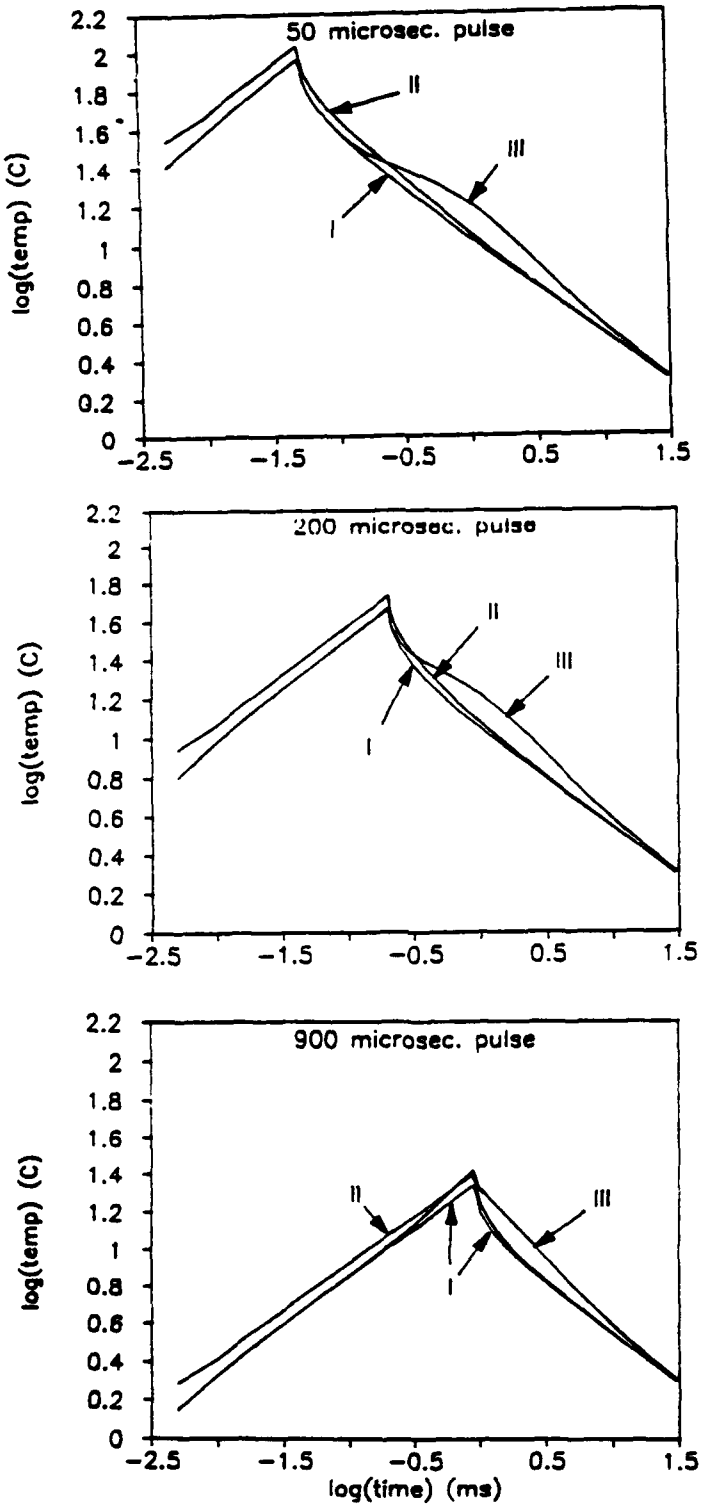

Figure 2. Finite difference calculation of ln(T) versus ln(t) for 50, 200, and 900 μs rectangular pulses incident on three different coating systems: (I) 137.5 μm chromium on steel; (II) 137.5 μm "low density" chromium on steel; and (III) 112.5 μm chromium on a 25 μm "thermal barrier" on steel.

Measurement of Temperature Using Black-Body Radiation

All objects emit electromagnetic radiation due to the thermal excitation of electrons in the molecules of the object. This radiation can be detected and used to measure the temperature of the object emitting the radiation.

Theoretical calculations of the intensity of such radiation as a function of wavelength or frequency can be made for an ideal black body--an object that absorbs all electromagnetic radiation incident upon it. The theory is fairly straightforward and can be found in introductory texts on modern physics or quantum optics (refs 4,5). The theoretical result is often written as

$$I_\nu(\nu) = \frac{2\pi h\nu^3}{c^2} \frac{1}{e^{h\nu/kT} - 1} \tag{7}$$

where $I_\nu(\nu)d\nu$ is the intensity of emitted radiation having frequencies between ν and $\nu + d\nu$, h is Planck's constant, k is Boltzmann's constant, and c is the speed of light in vacuum. T is the absolute temperature of the body.

However, one can also define $I_\lambda(\lambda)d\lambda$ as the intensity of emitted radiation having frequencies between λ and $\lambda + d\lambda$. By requiring $I_\lambda(\lambda)d\lambda = I_\nu(\nu)d\nu$, one can then obtain

$$I_\lambda(\lambda) = \frac{2\pi hc^2}{\lambda^5} \frac{1}{e^{hc/k\lambda T} - 1} \tag{8}$$

Some potential for confusion exists because $I_\lambda(\lambda)$ and $I_\nu(\nu)$ are not the same. $I_\lambda(\lambda)$ can be thought of as an intensity per unit wavelength, whereas $I_\nu(\nu)$ is an intensity per unit frequency.

Figure 3 shows $I_\lambda(\lambda)$ versus λ for several temperatures near room temperature. Near room temperature, virtually all of the black-body radiation is emitted in the infrared region of the spectrum, at wavelengths longer than those of visible light. Although a small amount of this black-body radiation is in the visible range, the human eye can not perceive it at such a low intensity. Virtually all the light that we see from objects at room temperature is either reflected from other sources or emitted by other mechanisms, such as electronic transitions, including luminescence, fluorescence, lasing, and electron-hole recombination. As the temperature of an object increases, it emits more black-body radiation at shorter wavelengths. If the temperature is raised high enough, the black-body radiation becomes easily visible to the naked eye, as with molten metal or the filament of an incandescent light bulb.

Not all materials, however, behave as ideal black bodies. At a given temperature and for radiation at a given wavelength, the ratio of actual intensity emitted to the intensity that would be emitted by an ideal black-body is called the spectral emittance. An ideal black body has an emittance of 1. All other materials have smaller values, although many have values very close to 1. The emittance of a particular material depends largely on its surface characteristics, such as roughness and the presence of an oxide. Most nonmetallic and painted surfaces have an emittance greater than 0.8. Near room temperatures, a highly polished metallic surface may have an emittance smaller than 0.05 for infrared wavelengths. Although polished chromium may have an emittance of about 0.1, unpolished LC chromium would have a significantly higher emittance.

A wide variety of detectors and scanners are available to detect infrared black-body radiation and measure a wide range of temperatures. In choosing a detector or scanner, one must consider its temperature range and sensitivity, the rate at which independent measurements can be made, the ease with

which the output signal can be converted to temperature, and the ability to correct for varying emittance. Most video-rate scanners are too slow to measure the type of temperature versus time profiles expected on chromium-coated steel. An exception might be made for the case of video scanners that can be converted to scan a single line of the object, rather than an area, at a much higher rate, such as 2500 lines per second. For the best time resolution, however, one should choose an infrared detector, such as indium antimonide (InSb), focused to a stationary spot on the surface.

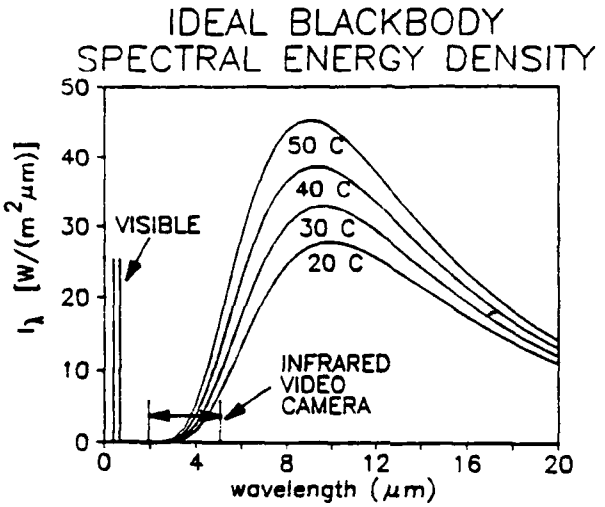

Figure 3. $I_\lambda(\lambda)$ versus λ.

ULTRASONIC TECHNIQUE

Principle

The ultrasonic approach attempts to detect and measure the interference between ultrasonic stress waves reflected from the chromium-steel interface and the chromium-air interface, as shown schematically in Figure 4. A reflection of stress waves will occur at an interface between media of different characteristic impedance. The characteristic impedance is defined as $z = \rho v$, where ρ is the density and v is the velocity of the stress wave in the medium. Normally, chromium and steel have very similar impedances, so that one would not expect a reflection at their interface. However, a poor bond or low density chromium coating might result in a significant discontinuity in impedance, and therefore, some measurable reflection.

Upon reflection, a stress wave will undergo either no phase shift or a phase shift of 180 degrees, depending upon whether the wave is longitudinal or shear and whether the impedance increases or decreases at the interface. For shear waves, no phase shift will occur if the incident medium has the higher impedance; if the incident medium has the lower impedance, a 180-degree phase shift will occur. For longitudinal waves, a phase shift of 180 degrees will occur if the incident medium has the higher impedance. For all practical purposes, air has an impedance of zero.

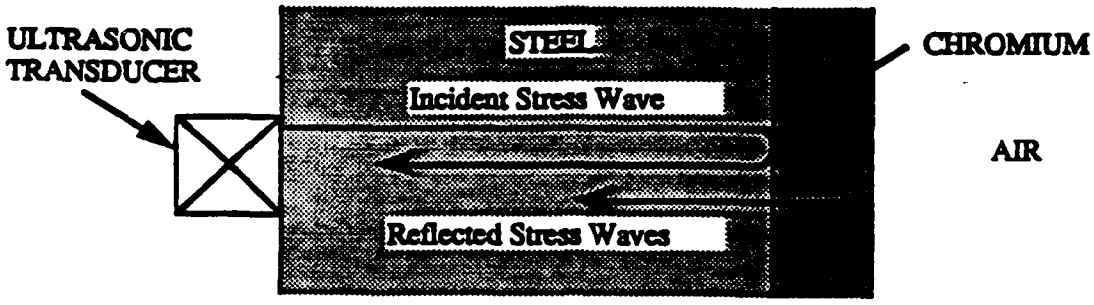

Figure 4. Reflection of ultrasonic stress waves from the chromium-steel interface and the chromium-air interface, assuming a discontinuity in characteristic impedance at the chromium-steel interface.

Therefore, destructive interference could occur in either of the following situations:

1. If the chromium had a lower impedance and its thickness was $(2n-1)\lambda/4$.

2. If the chromium had a higher impedance and its thickness was $n\lambda/2$, where n is a positive integer and λ is the wavelength of the stress wave in the chromium.

For a given thickness, the lowest frequency cases would occur for n = 1. The chromium in case #1, with the lower impedance, would then be analogous to an optical quarter-wave layer used as an anti-reflective coating. The chromium in case #2, with the higher impedance, would be a half-wave layer.

In the quarter-wave case, the frequency at which destructive interference occurs would be f = v/(4d), where v is the velocity of the wave in the chromium and d is the thickness of the chromium. In the half-wave case, destructive interference would occur at f = v/(2d). For purposes of predicting the frequency for which these interference effects would occur, one can assume a shear wave velocity of about 3200 m/s and a longitudinal wave velocity of about 5900 m/s. For shear waves reflected from a 125 μm coating, destructive interference should occur at 6.4 MHz for the quarter-wave case and 12.8 MHz for the half-wave case. For longitudinal waves reflected from a 125 μm coating, destructive interference should occur at 11.8 MHz for the quarter-wave case and 23.6 MHz for the half-wave case.

Specimen Preparation

Three bars, 15.5 by 25 by 112 mm, were cut from C1018 carbon steel. Two cylinders, 25 mm in diameter and 12.5 mm high, were cut from a length of oxygen-free, high conductivity (OFHC) CDA101 hard drawn copper rod. The copper cylinders were then annealed at 400°C for 50 minutes. One 25 by 112 mm face of each steel bar was polished with 400 and 600 grit silicon carbide, followed by 7 μm of diamond paste. The flat faces of the copper cylinders were similarly polished.

About 125 μm of LC chromium was electrodeposited onto the clean, polished surfaces of one steel bar and one copper cylinder. Another steel bar was prepared by first forming a thick oxide on the surface by heating at 250°C for about 90 minutes, then electrodepositing 125 μm of LC chromium over the oxidized surface that had previously been polished. In this case, the desire was to form a poorly bound coating that might result in stress wave reflection at the interface. The remaining steel bar and copper cylinder were left uncoated.

Results

Experimental evidence of interference was sought by measuring the effective attenuation of stress waves propagated from the uncoated side of the specimen and reflected from the coating, as shown in Figure 4. Data were collected using a computer-controlled velocity and attenuation measuring system (Matec Instruments, Model MBS-8000). The stress waves were sinusoidally varying "tone bursts" of 3 μs duration. A 5 MHz, 0.25-inch diameter transducer introduced shear waves into the specimen and received echoes. It was coupled to the surface using a viscous resin. A 10-MHz, 0.25-inch diameter transducer coupled to the surface with a fluid couplant introduced longitudinal waves and received echoes. Measurements were made for shear waves between 5 and 7 MHz and for longitudinal waves between 7 and 16 MHz. None of the measurements, however, appeared to show an increased attenuation due to destructive interference of waves reflected from the coating, although there was considerable variation with frequency, presumably due to the properties of steel. Figure 5 shows a plot of attenuation versus frequency for longitudinal waves in the three steel specimens.

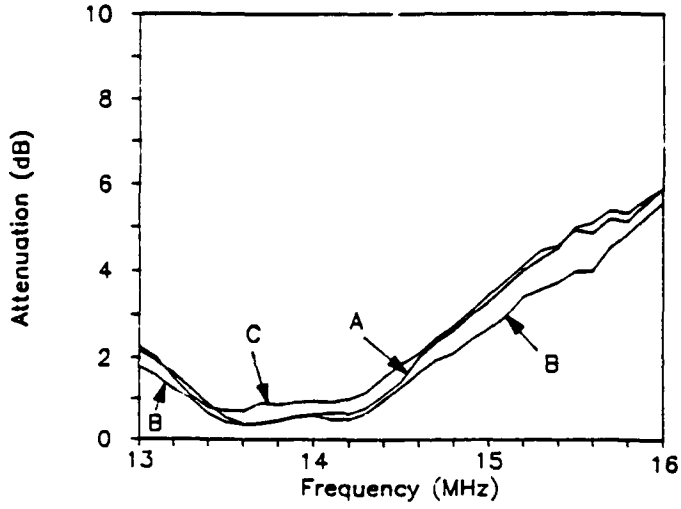

Figure 5. Attenuation of longitudinal stress waves reflected from (A) free steel surface, (B) clean steel with LC chromium, and (C) oxidized steel with LC chromium.

CONCLUSION

Although no conclusive experimental evidence was obtained in this study, photothermal and ultrasonic techniques appear to offer enough promise to justify pursuing further work.

REFERENCES

1. P. Cielo, "Pulsed Photothermal Evaluation of Layered Materials," *Journal of Applied Physics*, Vol. 56, No. 1, 1 July 1984, p. 230.

2. H.S. Carslaw and J.C. Jaeger, *Conduction of Heat in Solids*, Oxford University Press, London, 1959.

3. G.M. Dusinberre, *Heat-Transfer Calculations by Finite Differences*, International Textbook Co., Scranton, PA, 1961.

4. J.D. McGervey, *Introduction to Modern Physics*, Academic Press, New York, 1971.

5. R. Loudon, *The Quantum Theory of Light*, Clarendon Press, Oxford, 1983.

TECHNICAL REPORT INTERNAL DISTRIBUTION LIST

	NO. OF COPIES
CHIEF, DEVELOPMENT ENGINEERING DIVISION	
ATTN: SMCAR-CCB-DA	1
-DC	1
-DI	1
-DR	1
-DS (SYSTEMS)	1
CHIEF, ENGINEERING SUPPORT DIVISION	
ATTN: SMCAR-CCB-S	1
-SD	1
-SE	1
CHIEF, RESEARCH DIVISION	
ATTN: SMCAR-CCB-R	2
-RA	1
-RE	1
-RM	1
-RP	1
-RT	1
TECHNICAL LIBRARY	5
ATTN: SMCAR-CCB-TL	
TECHNICAL PUBLICATIONS & EDITING SECTION	3
ATTN: SMCAR-CCB-TL	
OPERATIONS DIRECTORATE	1
ATTN: SMCWV-ODP-P	
DIRECTOR, PROCUREMENT DIRECTORATE	1
ATTN: SMCWV-PP	
DIRECTOR, PRODUCT ASSURANCE DIRECTORATE	1
ATTN: SMCWV-QA	

NOTE: PLEASE NOTIFY DIRECTOR, BENET LABORATORIES, ATTN: SMCAR-CCB-TL, OF ANY ADDRESS CHANGES.

TECHNICAL REPORT EXTERNAL DISTRIBUTION LIST

	NO. OF COPIES
ASST SEC OF THE ARMY RESEARCH AND DEVELOPMENT ATTN: DEPT FOR SCI AND TECH THE PENTAGON WASHINGTON, D.C. 20310-0103	1
ADMINISTRATOR DEFENSE TECHNICAL INFO CENTER ATTN: DTIC-FDAC CAMERON STATION ALEXANDRIA, VA 22304-6145	12
COMMANDER US ARMY ARDEC ATTN: SMCAR-AEE	1
SMCAR-AES, BLDG. 321	1
SMCAR-AET-O, BLDG. 351N	1
SMCAR-CC	1
SMCAR-CCP-A	1
SMCAR-FSA	1
SMCAR-FSM-E	1
SMCAR-FSS-D, BLDG. 94	1
SMCAR-IMI-I (STINFO) BLDG. 59 PICATINNY ARSENAL, NJ 07806-5000	2
DIRECTOR US ARMY BALLISTIC RESEARCH LABORATORY ATTN: SLCBR-DD-T, BLDG. 305 ABERDEEN PROVING GROUND, MD 21005-5066	1
DIRECTOR US ARMY MATERIEL SYSTEMS ANALYSIS ACTV ATTN: AMXSY-MP ABERDEEN PROVING GROUND, MD 21005-5071	1
COMMANDER HQ, AMCCOM ATTN: AMSMC-IMP-L ROCK ISLAND, IL 61299-6000	1
COMMANDER ROCK ISLAND ARSENAL ATTN: SMCRI-ENM ROCK ISLAND, IL 61299-5000	1
DIRECTOR US ARMY INDUSTRIAL BASE ENGR ACTV ATTN: AMXIB-P ROCK ISLAND, IL 61299-7260	1
COMMANDER US ARMY TANK-AUTMV R&D COMMAND ATTN: AMSTA-DDL (TECH LIB) WARREN, MI 48397-5000	1
COMMANDER US MILITARY ACADEMY ATTN: DEPARTMENT OF MECHANICS WEST POINT, NY 10996-1792	1
US ARMY MISSILE COMMAND REDSTONE SCIENTIFIC INFO CTR ATTN: DOCUMENTS SECT, BLDG. 4484 REDSTONE ARSENAL, AL 35898-5241	2
COMMANDER US ARMY FGN SCIENCE AND TECH CTR ATTN: DRXST-SD 220 7TH STREET, N.E. CHARLOTTESVILLE, VA 22901	1
COMMANDER US ARMY LABCOM MATERIALS TECHNOLOGY LAB ATTN: SLCMT-IML (TECH LIB) WATERTOWN, MA 02172-0001	2

NOTE: PLEASE NOTIFY COMMANDER, ARMAMENT RESEARCH, DEVELOPMENT, AND ENGINEERING CENTER, US ARMY AMCCOM, ATTN: BENET LABORATORIES, SMCAR-CCB-TL, WATERVLIET, NY 12189-4050, OF ANY ADDRESS CHANGES.

TECHNICAL REPORT EXTERNAL DISTRIBUTION LIST (CONT'D)

	NO. OF COPIES
COMMANDER US ARMY LABCOM, ISA ATTN: SLCIS-IM-TL 2800 POWDER MILL ROAD ADELPHI, MD 20783-1145	1
COMMANDER US ARMY RESEARCH OFFICE ATTN: CHIEF, IPO P.O. BOX 12211 RESEARCH TRIANGLE PARK, NC 27709-2211	1
DIRECTOR US NAVAL RESEARCH LAB ATTN: MATERIALS SCI & TECH DIVISION CODE 26-27 (DOC LIB) WASHINGTON, D.C. 20375	1 1
DIRECTOR US ARMY BALLISTIC RESEARCH LABORATORY ATTN: SLCBR-IB-M (DR. BRUCE BURNS) ABERDEEN PROVING GROUND, MD 21005-5066	1
COMMANDER AIR FORCE ARMAMENT LABORATORY ATTN: AFATL/MN EGLIN AFB, FL 32542-5434	1
COMMANDER AIR FORCE ARMAMENT LABORATORY ATTN: AFATL/MNF EGLIN AFB, FL 32542-5434	1
MIAC/CINDAS PURDUE UNIVERSITY 2595 YEAGER ROAD WEST LAFAYETTE, IN 47905	1

NOTE: PLEASE NOTIFY COMMANDER, ARMAMENT RESEARCH, DEVELOPMENT, AND ENGINEERING CENTER, US ARMY AMCCOM, ATTN: BENET LABORATORIES, SMCAR-CCB-TL, WATERVLIET, NY 12189-4050, OF ANY ADDRESS CHANGES.